

Synthesis, Characterization and Catalytic Performance of Ti-Containing Mesoporous Molecular Sieves Assembled from Titanosilicate Precursors

Changzi Jin, Gang Li,* Xiangsheng Wang, Lixia Zhao, Liping Liu, and Haiou Liu

Department of Catalytical Chemistry and Engineering, State Key Laboratory of Fine Chemicals, Dalian University of Technology, Dalian, 116012, P.R. China

Yong Liu, Weiping Zhang, Xiuwen Han, and Xinhe Bao

State Key Laboratory of Catalysis, Dalian Institute of Chemical Physics, The Chinese Academy of Sciences, Dalian, 116023, P.R. China

Received October 29, 2006. Revised Manuscript Received February 6, 2007

Novel Ti-containing mesoporous materials with wormhole structure (Ti-WMS) can be assembled from preformed titanosilicate-1 precursors with long-chain alkylamines as structure directors. The obtained products were characterized by a series of techniques including powder X-ray diffraction, transmission electron microscopy, FT-infrared spectroscopy, UV–visible spectroscopy, N₂ sorption, and hyperpolarized ¹²⁹Xe NMR at variable temperature. The catalytic properties of the materials were investigated by oxidative desulfurization reactions. The results show that Ti-WMS, whose synthesis utilizes zeolite precursors as total or part of the silica and titanium sources, is a pure mesoporous phase. However, the prepared materials contain additional micropores except the uniform mesopores, which is confirmed by N₂ sorption and ¹²⁹Xe NMR. Infrared spectra indicate that there are zeolitic primary and secondary building units in the pore walls of Ti-WMS. UV–visible spectroscopy results confirm the existence of active Ti⁴⁺ species. Ti-WMS is very active in the oxidation of bulky sulfides such as benzothiophene, dibenzothiophene, and 4,6-dimethyl dibenzothiophene, with activities similar to Ti-HMS. However, in thiophene oxidation, which is not diffusion-limited, Ti-WMS exhibits much higher catalytic activity than Ti-HMS because of the presence of micropores and zeolite-like active sites.

1. Introduction

Ti-containing molecular sieves are effective catalysts for the selective oxidation of organic compounds. Traditional Ti-containing zeolites with crystalline structure have strong oxidation ability and high stability.^{1–9} However, an obvious shortcoming of this kind of catalyst is that its framework pores are too small to be accessed by bulky reactants, which prevent its wide use in fine chemical and petrochemical processing. Ti-containing mesoporous silicas possess a large pore size and high specific surface and show better performance than zeolitic catalysts for the conversion of bulky reactants.^{10–16} But the relative lower oxidation ability of these mesoporous molecular sieves, arising from the amorphous

nature of their frameworks, make them inactive in some reactions.¹⁷ In addition, regardless of the reactant accessibility, the capacious pores of these mesoporous materials compromise their shape-selective catalytic performance in the oxidation of small molecules. Therefore, synthesizing porous inorganic materials possessing multiple dimensions with highly active sites is significant.^{18–25}

* To whom correspondence should be addressed. Tel: +86-411-8368-9065. Fax: +86-411-8368-9065. E-mail: liganghg@dlut.edu.cn.

- (1) Taramasso, M.; Perego, G.; Notari, B. U.S. Patent 4410501, 1983.
- (2) Thangaraj, A.; Sivasanker, S. *J. Chem. Soc., Chem. Commun.* **1992**, 123.
- (3) Tuel, Z. *Zeolites* **1995**, *15*, 236.
- (4) Serrano, D. P.; Li, H. X.; Davis, M. E. *J. Chem. Soc., Chem. Commun.* **1992**, 745.
- (5) Cambor, M. A.; Corma, A.; Perez-Pariente, J. *Zeolite* **1993**, *13*, 82.
- (6) Cambor, M. A.; Constantini, A.; Corma, A.; Gilbert, L.; Esteve, P.; Martinez, A.; Valencia, S. *J. Chem. Soc., Chem. Commun.* **1996**, 1339.
- (7) Blasco, T.; Cambor, M. A.; Corma, A.; Perez-Pariente, J. *J. Am. Chem. Soc.* **1993**, *115*, 11806.
- (8) Huybrechts, D. R. C.; De Bruycker, L.; Jabobs, P. A. *Nature* **1990**, *345*, 240.
- (9) Roberts, M. A.; Sankar, G.; Thomas, J. M.; Jones, R. H.; Du, H.; Chen, J.; Pang, W.; Xu, R. *Nature* **1996**, *381*, 401.

- (10) Corma, A.; Navarro, M. T.; Pérez-Pariente, J. *J. Chem. Soc., Chem. Commun.* **1994**, 147.
- (11) Koyano, K. A.; Tatsumi, T. *Chem. Commun.* **1996**, 145.
- (12) Tanev, P. T.; Chibwe, M.; Pinnavaia, T. J. *Nature* **1994**, *368*, 321.
- (13) Zhang, W.; Wang, J.; Tanev, P. T.; Pinnavaia, T. J. *Chem. Commun.* **1996**, 979.
- (14) Zhang, W.; Froba, M.; Wang, J.; Tanev, P. T.; Wong, J.; Pinnavaia, T. J. *J. Am. Chem. Soc.* **1996**, *118*, 9164.
- (15) Bagshaw, S. A.; Renzo, F. D.; Fajula, F. *Chem. Commun.* **1996**, 2209.
- (16) Zhao, D.; Feng, J.; Huo, Q.; Melosh, N.; Fredrickson, G. H.; Chmelka, B. F.; Stucky, G. D. *Science* **1998**, *279*, 548.
- (17) Corma, A. *Chem. Rev.* **1997**, *97*, 2373.
- (18) Trong On, D.; Litic, D.; Kaliaguine, S. *Microporous Mesoporous Mater.* **2001**, *44–45*, 435.
- (19) Poladi, R. H. P. R.; Landry, C. C. *Microporous Mesoporous Mater.* **2002**, *52*, 11.
- (20) Xiao, F.-S.; Han, Y.; Yu, Y.; Meng, X.; Yang, M.; Wu, S. *J. Am. Chem. Soc.* **2002**, *124*, 888.
- (21) Meng, X.; Li, D.; Yang, X.; Yu, Y.; Wu, S.; Han, Y.; Yang, Q.; Jiang, D.; Xiao, F.-S. *J. Phys. Chem. B* **2003**, *107*, 8972.
- (22) Yang, X.; Han, Y.; Lin, K.; Tian, G.; Feng, Y.; Meng, X.; Di, Y.; Du, Y.; Zhang, Y.; Xiao, F.-S. *Chem. Commun.* **2004**, 2612.
- (23) Lin, K.; Sun, Z.; Lin, S.; Jiang, D.; Xiao, F.-S. *Microporous Mesoporous Mater.* **2004**, *72*, 193.
- (24) Schmidt, I.; Krogh, A.; Wienberg, K.; Carlsson, A.; Brorson, M.; Jacobsen, C. J. H. *Chem. Commun.* **2000**, 2157.

The published progress in this general field has involved primarily several routes to prepare “composite materials”, which are intended to combine the advantages of micro- and mesoporous molecular sieves. One is partial transformation of amorphous framework walls of conventional mesoporous titanium silicas into zeolitic crystals.^{18,19} However, this method is only applicable to those mesoporous materials with thicker pore walls and it is inevitable that the intrinsic mesostructure of the substrate, during the transformation process, is destroyed to a certain extent. Another interesting strategy is the direct assembly of mesostructural material using protozeolitic nanoclusters (zeolite seeds).^{20–23} The primary and secondary building units of the zeolite crystal, as well as the zeolite-like active sites, can be introduced into the mesoporous walls through this approach. As a result, a mesoporous material with high oxidation ability and hydrothermal stability can be obtained. In addition, there has been great development in the technique to synthesize zeolites with larger pores, which favor the diffusion of bulky reactants.^{24,25} In this contribution, we report a novel Ti-containing mesoporous molecular sieve, denoted as Ti-WMS, assembled by preformed TS-1 precursors and long-chain alkylamine. Moreover, for the convenience of distinguishing this material from conventional Ti-HMS, a series of samples can be obtained by utilizing TS-1 precursors and direct mixed gel of tetraethylorthosilicate and tetrabutylorthotitanate as silica and titanium sources together. We demonstrate that Ti-WMS exhibits a pure mesoporous phase, while possessing micropores. Different from Ti-HMS, Ti-WMS samples are active in the oxidation of both bulky and small sulfur compounds.

2. Experimental Section

Materials. Tetrabutylorthotitanate (TBOT), dodecylamine (DDA), and thiophene (Th) were purchased from Shanghai Chemical Co. Tetraethylorthosilicate (TEOS), ethanol, isopropyl alcohol (IPA), *n*-octane, and H₂O₂ (30 wt %) were purchased from Tianjin Kermel Chemical Co. Benzothiophene (BT), dibenzothiophene (DBT), and 4,6-dimethyl dibenzothiophene (4,6-DMDBT) were purchased from Acros Organics Co. Tetrapropylammonium hydroxide (TPAOH) was made by us through ion exchange process.

Synthesis. The synthesis procedure of Ti-WMS samples consists of a two-step process: (1) 11.2 mL of TEOS, 0.34 g of TBOT, 3.8 mL of IPA, 23.5 mL of TPAOH solution (0.64 M), and 5.4 mL of H₂O were mixed in this order to form a homogeneous solution with molar ratios of SiO₂/TiO₂/TPAOH/IPA/H₂O at 1.0/0.02/0.30/1.0/30. The mixture was heated at 40–50 °C for 3 h to remove the alcohol, followed by supplementing water to retain the original volume. Then the mixture was transferred into a stainless-steel Teflon-lined autoclave and aged at 80 °C for 15–24 h under static conditions. Thus, a titanosilicate precursor with TS-1 nanocrystals was prepared. (2) DDA (2.0 g) was dissolved in 19 mL of ethanol, followed by the addition of the TS-1 precursors obtained in step one under stirring. The pH value of the mixture was adjusted to 9–11 with HCl (3 M). The stirring was maintained at room temperature for 9–24 h, and the resulting solid was collected by filtration, washed with abundant distilled water, dried at 100 °C, and calcined at 640 °C for 5 h to remove the organic template. In addition, the use of TS-1 precursors and a direct mixed gel of TEOS

Table 1. Synthesis Gel and Material Compositions for Ti-HMS and Ti-WMS Samples

sample	precursors/ DDA ^a	ST-gel/ DDA ^b	SiO ₂ /TiO ₂ ^c gel	SiO ₂ /TiO ₂ ^d material
Ti-HMS	0	4.6	50	41
Ti-WMS-1	1.1	3.5	50	38
Ti-WMS-2	2.3	2.3	50	36
Ti-WMS-3	3.5	1.1	50	34
Ti-WMS	4.6	0	50	40

^a Molar ratios of SiO₂ in TS-1 precursors with DDA. ^b Molar ratios of SiO₂ in ST-gel with DDA. ^c Molar ratios from starting gel. ^d Molar ratios from material analyzed by XRF.

and TBOT (ST-gel) as silica and titanium sources had also been adopted. The other conditions were the same as those described above and the obtained products were denoted as Ti-WMS-*n* (*n* = 1, 2, or 3). The difference in the *n* value represents that the products were synthesized from different proportions of TS-1 precursors and ST-gel. The detailed information of the synthesis is presented in Table 1.

For comparative purposes, a Ti-HMS sample was prepared with ST-gel as silica and titanium sources. The detailed synthesis procedure can be referred to in the published literature.¹³ TS-1 was synthesized according to the literature.²

Characterization. Powder X-ray diffraction (XRD) patterns were recorded using a Rigaku D/Max 2400 diffractometer, which employed Cu K α radiation. Transmission electron microscopy (TEM) images were taken on Tecnai G² 20 S-twin instrument (FEI company) with an acceleration voltage of 200 kV. The nitrogen adsorption isotherm was measured using a Quantachrome AUTOSORB-1 physical adsorption apparatus. The pore size distribution was calculated by using the Barrett–Joyner–Halenda (BJH) model. FT-IR spectra were recorded on a Bruker EQUINOX55 spectrometer, using KBr pellet technique. UV–vis spectra were obtained on a JASCO UV550 spectrometer with BaSO₄ as the internal standard. The absorbency (*A*) was calculated from the intensity of incident light (*I*₀) and reflected light (*I*₁) according to the function $A = \log(I_0/I_1)$. The chemical compositions of the samples were obtained on a Bruker SRS-3400 sequential X-ray spectrometer (XRF). Continuous-flow hyperpolarized ¹²⁹Xe NMR spectra were collected on a Varian Infinityplus-400 spectrometer operating at 110.6 MHz with a recycle delay of 2 s, 90° pulse width of 3 μ s, and 400–1000 scans.

Catalytic Tests. An amount of sulfur compound (Th, BT, DBT, and 4,6-DMDBT) was dissolved in *n*-octane to act as model fuel, and the concentration of sulfide in the model fuel was about 1000 ppm. The reaction was performed under vigorous stirring in a three-neck glass flask with a water-bathed jacket. In a stand run, 10 mL of model fuel, 10 mL of solvent (methanol as solvent in BT, DBT, and 4,6-DMDBT oxidation; water as solvent in Th oxidation), and 100 mg of catalyst (no catalyst in blank examples) were added to the reactor. Ten microliters of H₂O₂ (30 wt %) was used as oxidant and the reaction was carried out at 333 K for 4–6 h. The oil phase was analyzed periodically by means of a GC HP6890 equipped with HP-5 capillary column (φ 0.32 mm \times 30 m) and a FPD detector. The removal rate (*R*) of sulfur compounds is expressed as

$$R = \frac{C_0 - C_t}{C_0} \times 100\%$$

*C*₀ is the initial mass concentration of sulfur compounds and *C*_{*t*} is the mass concentration after reacting *t* h.

3. Results and Discussions

3.1. Synthesis and Characterization of Materials. Figure 1 presents the powder X-ray diffraction (XRD) patterns of

(25) Tao, Y.; Kanoh, H.; Abrams, L.; Kaneko, K. *Chem. Rev.* **2006**, *106*, 896.

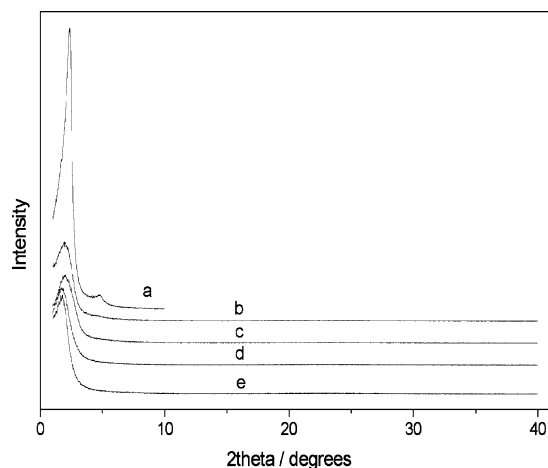


Figure 1. XRD patterns of calcined (a) Ti-HMS, (b) Ti-WMS-1, (c) Ti-WMS-2, (d) Ti-WMS-3, and (e) Ti-WMS.

Table 2. Structural Properties of Ti-HMS and Ti-WMS Samples

sample	d_{100}^a (nm)	a_0^b (nm)	pore size ^c (nm)	wall thickness ^d (nm)	BET surface area (m ² /g)	total pore volume ^e (cm ³ /g)	micropore volume ^f (cm ³ /g)
Ti-HMS	3.6	4.2	2.3	1.9	829.7	0.69	
Ti-WMS-1	4.3	5.0	2.3	2.7	854.4	0.79	0.01
Ti-WMS-2	4.3	5.0	2.3	2.7	761.0	0.77	0.02
Ti-WMS-3	4.9	5.7	2.3	3.4	754.3	0.77	0.03
Ti-WMS	4.9	5.7	2.3	3.4	761.3	0.89	0.03

^a Calculated from XRD analysis. ^b $a_0 = 2d_{100}/3^{1/2}$. ^c Calculated from adsorption branch of nitrogen isotherm using BJH model. ^d Wall thickness = a_0 - pore size. ^e Calculated from the volume adsorbed of P/P_0 at 0.99. ^f Calculated from t -plots analysis.

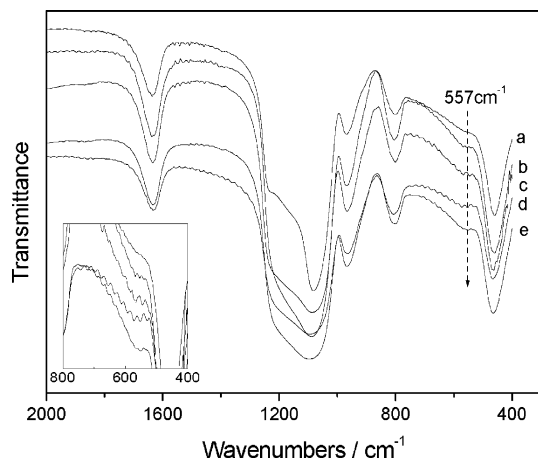


Figure 2. FT-IR spectra of calcined (a) Ti-HMS, (b) Ti-WMS-1, (c) Ti-WMS-2, (d) Ti-WMS-3, and (e) Ti-WMS. Inset: magnified for the region of 400–800 cm⁻¹.

the samples. All of the patterns contain an intense diffraction peak (reflection 100) in the low-angle region. For Ti-HMS, an additional weak broad shoulder near 5° can be seen, which is absent in the XRD patterns of the Ti-WMS samples. The results show that all samples have typical wormhole structure and that the Ti-WMS samples assembled from the TS-1 precursors have a lower degree of structure order than Ti-HMS assembled from ST-gel.²⁶ It can also be found from the XRD analysis that, relative to Ti-HMS, the Ti-WMS samples reflect a larger d_{100} value (Table 2) and lower intensity of the (100) diffraction peaks. In addition, with

(26) Zhang, W.; Pauly, T. R.; Pinnavaia, T. J. *Chem. Mater.* **1997**, *9*, 2491.

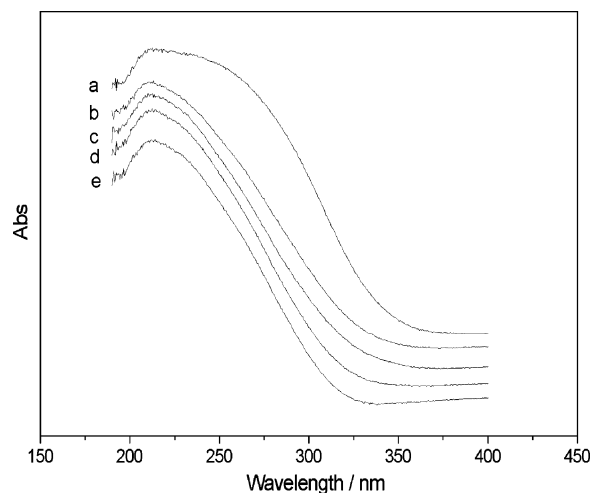


Figure 3. UV-visible spectra of calcined (a) Ti-HMS, (b) Ti-WMS-1, (c) Ti-WMS-2, (d) Ti-WMS-3, and (e) Ti-WMS.

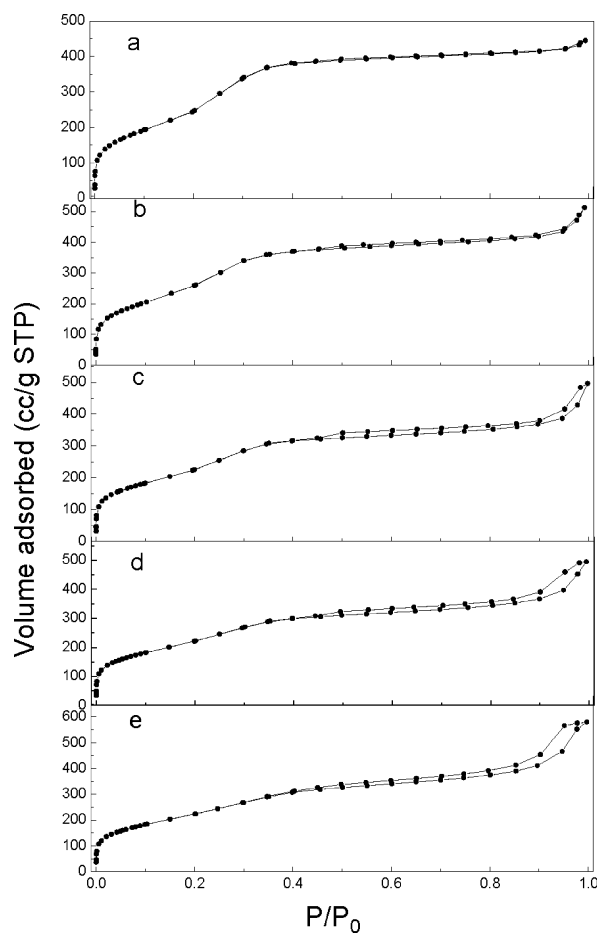


Figure 4. Nitrogen adsorption isotherms of calcined (a) Ti-HMS, (b) Ti-WMS-1, (c) Ti-WMS-2, (d) Ti-WMS-3, and (e) Ti-WMS.

increasing amount of TS-1 precursors in the synthesis of Ti-WMS samples, the corresponding d_{100} value increases too. These results can be attributed to the larger volumes and stronger rigidity of TS-1 nanocrystals in the TS-1 precursors relative to ST-gel species.^{27–29} No diffraction peaks were

(27) de Moor, P. E. A.; Beelen, T. P. M.; van Santen, R. A. *J. Phys. Chem. B* **1999**, *103*, 1639.

(28) Kirschhock, C. E. A.; Ravishankar, R.; Verspeurt, F.; Grobet, P. J.; Jacobs, P. A.; Martens, J. A. *J. Phys. Chem. B* **1999**, *103*, 4965.

(29) Kirschhock, C. E. A.; Ravishankar, R.; Jacobs, P. A.; Martens, J. A. *J. Phys. Chem. B* **1999**, *103*, 11021.

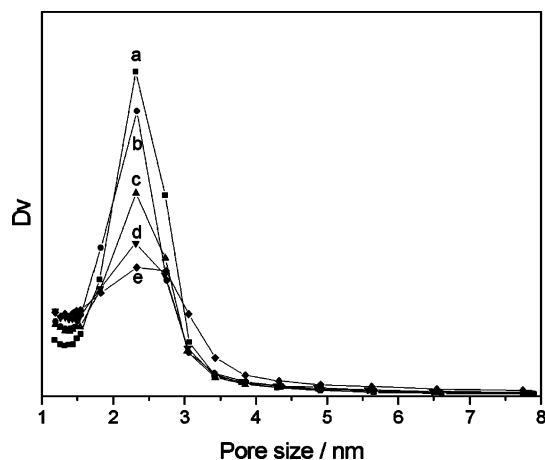


Figure 5. Pore size distributions of calcined (a) Ti-HMS, (b) Ti-WMS-1, (c) Ti-WMS-2, (d) Ti-WMS-3, and (e) Ti-WMS.

found in the wide-angle region in the XRD patterns. This reveals that all Ti-WMS samples are pure phase without large zeolite crystals. The same conclusion can be drawn from the TEM images (not shown) of the Ti-WMS samples.

Figure 2 shows FT-IR spectra of all calcined samples. There is no band in the region of $500\text{--}600\text{ cm}^{-1}$ in the IR spectrum of Ti-HMS, which is similar to other conventional mesoporous material. For the Ti-WMS samples, however, there is a band at approximately 557 cm^{-1} , which is characteristic of the vibration of the five-membered rings in zeolite crystals. A correlation can be observed between the intensity of the 557 cm^{-1} band and the amount of TS-1 precursors in the synthesis of Ti-WMS samples. With increasing amount of TS-1 precursors in the preparation process, from sample (b) to sample (e), the intensity of the 557 cm^{-1} band increases gradually. The result indicates that the Ti-WMS samples assembled from the TS-1 precursors contain basic zeolitic building units.

UV-visible spectroscopy is an effective method to characterize the nature and coordination of titanium ions in titanium-substituted material. Figure 3 gives the UV spectra of all Ti-HMS and Ti-WMS samples. All samples show an absorption peak at $210\text{--}220\text{ nm}$, which indicates the existence of framework Ti species in tetrahedral coordination, which is the active center of the titanium-substituted samples. The XRF analysis also confirmed the existence of Ti in Ti-HMS and Ti-WMS samples (Table 1). In addition, there are

no significant differences in Ti contents of Ti-HMS assembled from TS-gel and Ti-WMS samples assembled from TS-1 precursors. The UV spectra of the Ti-WMS samples are appreciably different from that of Ti-HMS. The Ti-HMS sample exhibits a broader band, just like other mesoporous molecular sieves with amorphous framework; however, the corresponding band in the spectra of the Ti-WMS samples are relatively sharper. This difference can be attributed to the fact that the Ti-WMS samples assembled from zeolite precursors possess crystal-like active sites.¹³ For all the samples, no band was found near 330 nm , which indicates the absence of anatase phase.

Figure 4 shows the nitrogen adsorption isotherms of the Ti-HMS and Ti-WMS samples. Notably, all samples show typical type-IV isotherms, with a step at a relative pressure of $0.2\text{--}0.4$, which indicates the presence of framework-confined mesopores with uniform dimension (Figure 5). From sample (a) to sample (e), the slope at P/P_0 of $0.2\text{--}0.4$ became less steep, which indicates that the uniformity of the pore size of Ti-WMS samples assembled from TS-1 precursors drops relative to the Ti-HMS assembled from ST-gel. This point has been proven by the pore size distribution of samples (Figure 5). Despite the fact that all samples exhibit the same average value of pore diameters (2.3 nm), as the contribution of TS-1 precursors in the synthesis increased, the pore size distributions of the products became broader. This result also indicates that the materials prepared from zeolitic precursors have disordered structure compared to the materials synthesized through conventional process. In addition, for the isotherms of Ti-WMS samples, another capillary condensation step at partial pressure >0.85 was observed, which indicates the filling of more larger interparticle pores. Because of this, the total pore volumes of Ti-WMS samples are larger than that of Ti-HMS (Table 2).

Figure 6 shows the t -plot curves of Ti-HMS and Ti-WMS. There are no micropores in Ti-HMS prepared through conventional process, which is confirmed by the fact that its t -plot curves pass through the origin (Figure 6a). Interestingly, Ti-WMS assembled from TS-1 precursors gives a micropore volume of $0.03\text{ cm}^3/\text{g}$. Similar results were found in Ti-WMS- n samples, which are shown in Table 2. It should be pointed out that, for the t -plot curves of both Ti-HMS and Ti-WMS, the first six points cut the vertical axis below

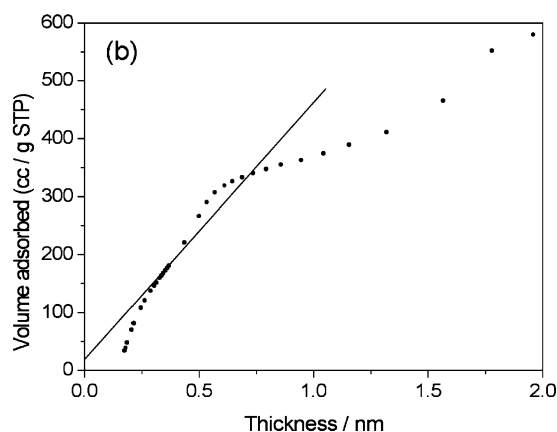
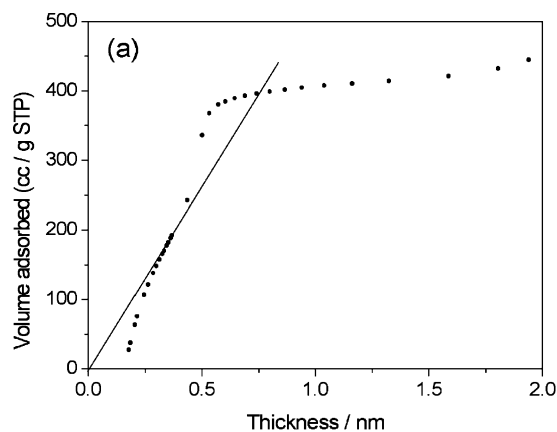


Figure 6. t -Plot curves of (a) Ti-HMS and (b) Ti-WMS.

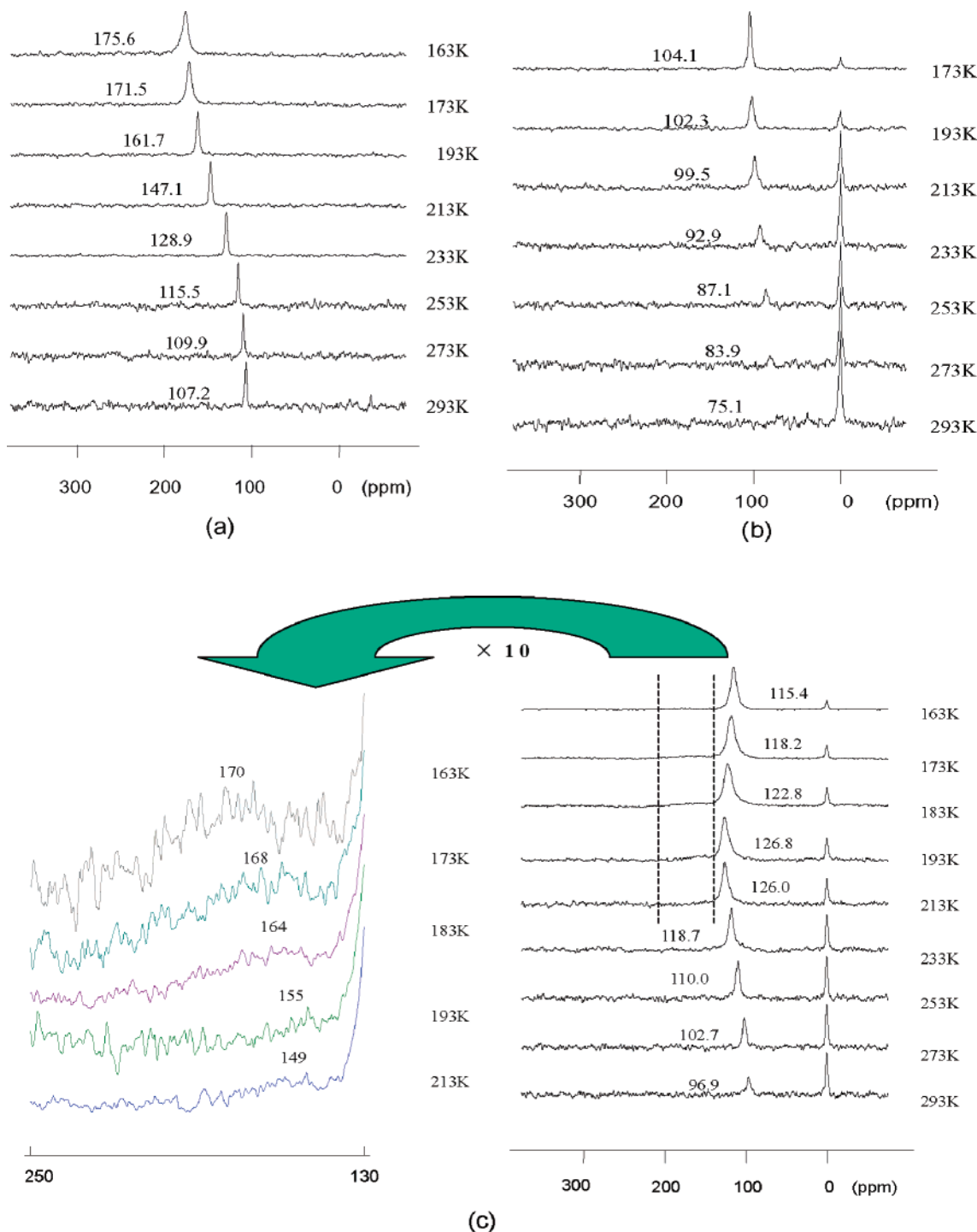


Figure 7. Hyperpolarized ^{129}Xe NMR spectra at variable temperatures of TS-1 (a), Ti-HMS (b), and Ti-WMS (c) samples.

the origin, which can be attributed to the presence of nonequilibrium points. In addition, it has been found from Table 2 that the Ti-WMS samples have larger wall thickness than the Ti-HMS. We propose the existence of micropores and the larger wall thickness in the Ti-WMS samples may be attributed to the existence of TS-1 building units in the mesoporous walls.

^{129}Xe NMR spectroscopy is a powerful technique for investigating porous structures of materials, especially samples with micropores.^{30–33} The high polarizability of its electron cloud make xenon very sensitive for physical interactions with its environment. In this study, the hyper-

polarized ^{129}Xe NMR technique was used to analyze the pore structure of Ti-WMS. Figure 7 presents the hyperpolarized ^{129}Xe NMR spectra of TS-1, Ti-HMS, and Ti-WMS samples. For the TS-1 sample (Figure 7a), the only signal at low field is associated with xenon absorbed in the micropores of TS-1

- (30) Bonardet, J.; Fraissard, J.; Gedeon, A.; Springuel-Huet, M. A. *Catal. Rev.-Sci. Eng.* **1999**, *41*, 115.
- (31) Zhang, W.; Han, X.; Liu, X.; Lei, H.; Bao, X. *Chem. Commun.* **2001**, 291.
- (32) Haake, M.; Pines, A.; Reimer, J. A.; Seydoux, R. *J. Am. Chem. Soc.* **1997**, *119*, 11711.
- (33) Zhang, W.; Ratcliffe, C. I.; Moudrakovski, I.; Mou, C.-Y.; Ripmeester, J. A. *Anal. Chem.* **2005**, *77*, 3379.

zeolite. The ^{129}Xe NMR spectra of Ti-HMS (Figure 7b) consist of two peaks. The peak at 0 ppm is from xenon in the gas phase and the peak at lower field is attributed to absorbed xenon in the mesochannels of the Ti-HMS molecular sieve. With decreasing temperature, the peak intensity of gaseous xenon reduced, while the signal of absorbed xenon in mesopores of Ti-HMS increased and shifted to low field. This is due to the fact that more and more gas-phase xenon will be condensed in the samples at lower temperatures, which increases the xenon–xenon interaction in the absorbed state. For the sample Ti-WMS, a main signal at low field is observed, which can be ascribed to the xenon adsorbed in the mesopores of Ti-WMS. In addition, another weak broad signal at lower field appears in ^{129}Xe NMR spectra of Ti-WMS when the temperature is lower than 213 K, which is similar to TS-1 and may be attributed to xenon adsorbed in micropores. In the ^{129}Xe NMR spectra of Ti-WMS sample (Figure 7c), the chemical shift of the signal at low field is clearly larger than that of Ti-HMS. This may be due to the exchange of xenon in different porous domains, e.g., the mesopores and micropores of Ti-WMS. The results further indicate that Ti-WMS assembled from zeolitic precursors contains micropores and is different from Ti-HMS prepared by the conventional method.

3.2. Catalysis. Generally, oxidative desulfurization was considered as one of the most promising alternative desulfurization processes to obtain ultralow sulfur fuels and many kinds of organic sulfur compounds can be removed effectively by the oxidative process.^{34–39} In this work, the catalytic performance of Ti-WMS samples was investigated by selective oxidation of various sulfur compounds, including Th, BT, DBT, and 4,6-DMDBT. Comparisons of the results were made with those of Ti-HMS and are exhibited in Figures 8–11.

Molecule accessibility and site activity are key elements in any reaction. For the oxidation of Th, Th being relatively small in size and highly stable, the requirement of a highly active site seems to be more essential than molecular accessibility for the catalyst. Therefore, Ti-HMS mesoporous molecular sieve with amorphous framework and resulting low oxidation ability cannot catalyze this reaction effectively, giving the final removal rate only at 33% (Figure 8). TS-1 exhibits excellent activity in this reaction, which is in good agreement with our previous reports. Interestingly, Ti-WMS gives a removal rate of 57% after 6 h, much higher than that of Ti-HMS. The catalytic activities of all Ti-WMS-*n* samples in Th oxidation have an advantage over Ti-HMS too. This can be due to the fact that the Ti-WMS samples were synthesized with TS-1 precursors as total or partial silica and titanium sources. The zeolite-like active sites and corresponding micropores can be introduced into mesoporous walls. As a result, the oxidation abilities and shape-selective

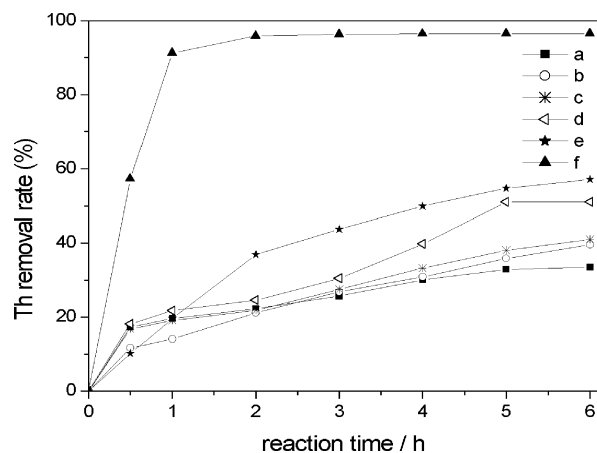


Figure 8. Catalytic performances of different samples in Th oxidation. (a) Ti-HMS; (b) Ti-WMS-1; (c) Ti-WMS-2; (d) Ti-WMS-3; (e) Ti-WMS; (f) TS-1.

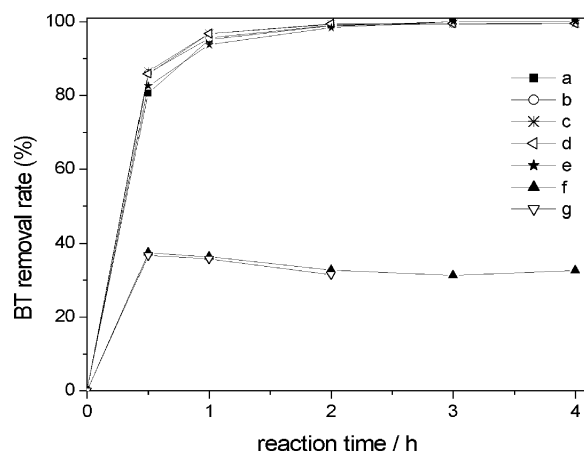


Figure 9. Catalytic performances of different samples in BT oxidation. (a) Ti-HMS; (b) Ti-WMS-1; (c) Ti-WMS-2; (d) Ti-WMS-3; (e) Ti-WMS; (f) TS-1; (g) blank.

properties of Ti-WMS series samples are predominant relative to Ti-HMS assembled from conventional ST-gel.

For BT, DBT, and 4,6-DMDBT, which possess a bulky volume, their oxidative reactions are diffusion-limited. In addition, these large organic sulfur compounds are easy to oxidize relative to Th because of their higher electron density on the sulfur atom. Therefore, the catalysts with large channels are first choice for reactions of these large molecules. Figures 9 and 10 present the catalytic performance of different catalysts in the oxidation of BT and DBT, respectively. Notably, all samples except the TS-1 are active in these two reactions. Even the Ti-HMS, which possesses low oxidation ability, gives a final removal rate of almost 100% and the reason is just as described above. 4,6-DMDBT has a larger size than DBT because of the existence of substituents at the fourth and sixth position. So the oxidation of 4,6-DMDBT demands more molecular accessibility. Figure 11 provides the results of different catalysts in the oxidation of 4,6-DMDBT. Ti-HMS exhibits the highest activity with a final removal percentage of 88%. The catalytic performances of the Ti-WMS samples in this reaction are a little lower than that of Ti-HMS. We propose that the reason is that the Ti-WMS samples assembled from TS-1 precursors contain micropores. Therefore, it is possible that a portion of the active centers (Ti^{4+}) exist in the micropores, which

(34) Reddy, R. S.; Reddy, J. S.; Kumar, R.; Kumar, P. *J. Chem. Soc., Chem. Commun.* **1992**, 84.

(35) Vasily, H.; Fajula, F.; Bousquet, J. *J. Catal.* **2001**, *198*, 179.

(36) Shiraishi, Y.; Hara, H.; Komosawa, I. *J. Chem. Eng. Jpn.* **2002**, *35*, 1305.

(37) Kong, L. Y.; Li, G.; Wang, X. S. *Catal. Today* **2004**, *93–95*, 341.

(38) Kong, L. Y.; Li, G.; Wang, X. S. *Catal. Lett.* **2004**, *92*, 163.

(39) Chica, A.; Corma, A.; Dómine, M. E. *J. Catal.* **2006**, *242*, 299.

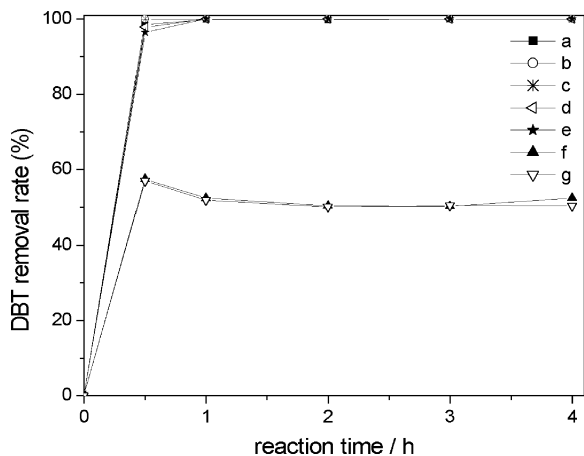


Figure 10. Catalytic performances of different samples in DBT oxidation. (a) Ti-HMS; (b) Ti-WMS-1; (c) Ti-WMS-2; (d) Ti-WMS-3; (e) Ti-WMS; (f) TS-1; (g) blank.

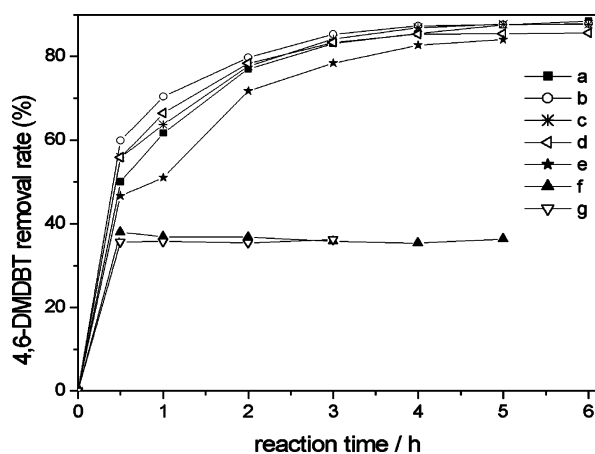


Figure 11. Catalytic performances of different samples in 4,6-DMDBT oxidation. (a) Ti-HMS; (b) Ti-WMS-1; (c) Ti-WMS-2; (d) Ti-WMS-3; (e) Ti-WMS; (f) TS-1; (g) blank.

leads to a reduction of active sites located in the mesopores relative to Ti-HMS. For 4,6-DMDBT oxidation, the active centers in micropores are nearly noneffective. This can be proved by the fact that TS-1 has no activity in this reaction. Because the dimensions of BT, DBT, and 4,6-DMDBT are larger than the pore size of TS-1, TS-1 is not active in their oxidation and the corresponding removal rates are in consequence of the extraction of solvent. Essentially, according to the reaction results, it is reasonable to expect that Ti-WMS would be superior to and surpass Ti-HMS and TS-1 in oxidative desulfurization of real fuel, which contains sulfur compounds of various sizes.

Just as described in the Introduction, the strategy of assembling mesoporous materials using preformed zeolite precursors has been a hot topic in recent years.^{20–23} In the published literature, MTS-5, MTS-8, and MTS-9 assembled from TS-1 precursors with cetyltrimethylammonium bromide or triblock copolymers exhibit high activities in a series of

oxidations.^{20,21,23} Among these materials, MTS-5 is synthesized in alkaline media at high temperature (100 °C).²³ Notably, not only the mesostructure will form but also the zeolitic seeds in preformed precursors easily grow into the zeolite phase under such conditions. Therefore, the synthesis of MTS-5 should be controlled carefully to avoid obtaining the mixture of mesostructure and zeolite. This problem has been solved effectively in the examples of MTS-8 and MTS-9, whose preparations are carried out in acidic system.^{21,23} However, there is another problem to be considered. The active sites of MTS-8 and MTS-9 synthesized under acidic conditions, relative to MTS-5, are not thermally stable, which prohibit their wide use. The Ti-WMS in our report was synthesized through the assembly of preformed TS-1 precursors with long-chain alkylamine at room temperature. Though the synthesis of Ti-WMS was also carried out in an alkaline system, the mild conditions of ambient temperature will prevent the TS-1 nanocrystals from growing into zeolite phase. In addition, the Ti-WMS has thermally stable active sites and exhibits high activity even after calcination at 640 °C for several hours. Therefore, compared to the rigorous synthesis conditions and weak thermal stability of the materials published previously, the Ti-WMS we report here has certain advantages.

4. Conclusion

A novel Ti-containing material (Ti-WMS), which possesses simultaneously mesopores and micropores and exhibits high catalytic activities in oxidative desulfurization, has been successfully synthesized through a two-step process. We propose that the particular structure and excellent catalytic performance of Ti-WMS is due to the fact that this material was prepared from preformed TS-1 precursors. This can be confirmed by the fact that the Ti-WMS-*n* samples, which were synthesized utilizing TS-1 precursors as partial silica and titanium sources, are similar to Ti-WMS. To be precise, the structural characteristic and catalytic activity of Ti-WMS-*n* samples are a cross between Ti-WMS and Ti-HMS. In contrast to other “composite materials” published previously, Ti-WMS with thermally stable active sites can be prepared at room temperature and the appearance of a mixture phase is easily avoided. Therefore, the concept of preparing Ti-containing mesoporous materials from preformed titanium silicate precursors has been extended to a new line of research by the synthesis of Ti-WMS.

Acknowledgment. The financial support of the Foundation for the Author of National Excellent Doctoral Dissertation of PR China (No. 200346), Program for New Century Excellent Talents in University (NCET-04-0270), National Natural Science Foundation of China (No. 20406005), and China National Petroleum Co. is gratefully acknowledged.